Potential impacts of two SO_2 oxidation pathways on regional sulfate concentrations: aqueous-phase oxidation by NO_2 and gas-phase oxidation by Stabilized Criegee Intermediates

Golam Sarwar[1]*, Kathleen Fahey[1], Roger Kwok[1], Shawn J. Roselle[1], Rohit Mathur[1], Jian Xue[2], Jianzhen Yu[2], William P. L. Carter[3]

[1]Atmospheric Modeling and Analysis Division, National Exposure Research Laboratory, U.S. Environmental Protection Agency, RTP, NC 27711, USA

[2] The Hong Kong University of Science & Technology, Clear Water bay, Kowloon, Hong Kong, China

[3]CE-CERT, University of California, Riverside, California 92521, USA

Corresponding author address: Golam Sarwar, US EPA, 109 T.W. Alexander Drive, Research Triangle Park, NC 27711, USA; Tel.: +1-919-541-2669; fax: +1-919-541-1379; *E-mail address*: sarwar.golam@epa.gov

Abstract

We examine the potential impacts of two additional sulfate production pathways using the Community Multiscale Air Quality modeling system. First we evaluate the impact of the aqueous-phase oxidation of S(IV) by nitrogen dioxide using two published rate constants, differing by 1-2 orders of magnitude. The reaction with alternate high and low rate constants enhances monthly mean wintertime sulfate by 4-20% and 0.4-1.2% respectively. The reaction does not significantly impact summertime sulfate. The higher sulfate predictions compare better with the observed data as the model tends to underpredict sulfate concentrations throughout the year. We also investigate the potential impact of the gas-phase oxidation of sulfur dioxide by the Stabilized Criegee Intermediate (SCI) using a recently measured rate constant for its reaction with sulfur dioxide. Initial tests indicate that the gas-phase oxidation of sulfur dioxide by the SCI does not significantly affect sulfate concentrations due to the competing reaction of the SCI with water vapor. The current estimate of the rate constant for the SCI reaction with water vapor is too high for the SCI reaction with sulfur dioxide to significantly affect sulfate production. However, a sensitivity analysis using a lower rate constant for the water vapor reaction suggests that the SCI reaction with sulfur dioxide could potentially enhance sulfate production in the model. Further study is needed to accurately measure the rate constants of the aqueous-phase oxidation of S(IV) by nitrogen dioxide and the gas-phase reaction of the SCI with water vapor.

Keywords: sulfate; aqueous chemistry; Criegee intermediate; SO_2; NO_2; alkene; O_3

1. Introduction

Sulfate (SO_4^{2-}) comprises a significant fraction of atmospheric particulate matter, and its relative atmospheric abundance has important implications for several environmental issues including acid rain, human and ecosystem health, and alteration of the earth's energy balance (due to scattering of incoming radiation). Particulate SO_4^{2-} can be emitted directly or produced in the atmosphere via gas- or aqueous-phase oxidation of sulfur dioxide (SO_2). The gas-phase oxidation of SO_2 by hydroxyl radical (OH) leads to the production of SO_4^{2-} in the atmosphere, and several aqueous-phase chemical pathways have been identified for the conversion of S(IV) (the sum of $SO_2 \cdot H_2O$ [hydrated SO_2], HSO_3^- [bisulfite ion] and SO_3^{2}[sulfite ion]) to SO_4^{2-} (Seinfeld and Pandis, 2006). These pathways include the aqueous-phase oxidation of S(IV) by hydrogen peroxide (H_2O_2), ozone (O_3), oxygen catalyzed by iron (Fe[III]) and manganese (Mn[II]), methylhydroperoxide (MHP), peroxyacetic acid (PAA), nitrogen dioxide (NO_2), as well as other oxidants. In environments where clouds or fogs are present, the production of SO_4^{2-} is often dominated by aqueous-phase oxidation of S(IV) by H_2O_2 or O_3 (Seigneur and Saxena, 1988).

In many models, the aqueous-phase oxidation of S(IV) by NO_2 is generally overlooked due to the limited water solubility of NO_2 (Seinfeld and Pandis, 2006). However, under certain conditions, this may be a significant S(IV) oxidation pathway, such as for fog events in areas with high NO_2 levels and sufficient neutralizing capacity (Pandis and Seinfeld,1989). There have been several studies of this reaction that indicate a range of rate constants that differ by 1-2 orders of magnitude depending on experimental conditions (Lee and Schwartz, 1983; Huie and Neta, 1986; Clifton et al., 1988). Lee and Schwartz (1983) reported a pH dependent rate constant of 1.4×10^5 - 2.0×10^6 $M^{-1}s^{-1}$ while Clifton et al. (1988) reported much greater values for the rate constant. Pandis and Seinfeld (1989) used the lower reaction rate constant proposed by Lee and Schwartz (1983). In a later study, Littlejohn et al. (1993) adopted the higher reaction rate by Clifton et al. (1988) and suggested SO_4^{2-} production from the reaction of S(IV) with dissolved NO_2 could be comparable to the contributions from the S(IV)-H_2O_2 reaction over a range of atmospheric conditions with high NO_2 concentrations and high aqueous phase pH.

Alkenes are emitted from both anthropogenic and biogenic sources. The reactions of alkenes and O_3 produce Criegee biradicals which can decompose or become Stabilized Criegee Intermediates (SCI) (Finlayson-Pitts and Pitts, 2000). The effect of the O_3-alkene reactions on SO_4^{2-} was first recognized in the early 70's when Cox and Penkett (1971) conducted experiments in a 220-liter aluminum chamber with O_3, alkenes, and SO_2. The O_3-alkene reactions increased SO_4^{2-} in the chamber. The reaction of O_3 with SO_2 proceeded at a very slow rate; thus, Cox and Penkett suggested that the O_3-alkene reactions form some intermediate which then reacts with SO_2 to form SO_4^{2-}. In a subsequent study, Cox and Penkett (1972) suggested that the presence of water vapor (H_2O) inhibits the oxidation of SO_2 by the O_3-alkene reactions. Calvert et al. (1978) suggested that the Criegee intermediate can oxidize SO_2 to form SO_4^{2-}. Calvert and Stockwell (1983) conducted box model simulations using known gas-phase chemistry and suggested that the reaction of SCI with SO_2 could enhance the SO_2 oxidation rate in highly polluted environments at low relative humidity. Hatakeyama and Akimoto (1994) conducted a review of the reactions of Criegee intermediates and noted that the reported rate constants vary from 3.0×10^{-15} to 1.7×10^{-11} cm^3 $molecule^{-1}$ s^{-1} for the

bimolecular reaction of SCI and SO_2, $1.0x10^{-17}$ to $7.0x10^{-13}$ cm^3 $molecule^{-1}$ s^{-1} for the bimolecular reaction of SCI and NO_2, and $2.0x10^{-19}$ to $1.0x10^{-15}$ for the bimolecular reaction of SCI and H_2O. It should be noted these values are based on estimates by different investigators since the technique to detect SCI did not exist. Welz et al. (2012) recently conducted direct kinetic measurements of the reactions of SCI with SO_2, NO_2, nitric oxide (NO), and H_2O and suggested that SCI can react with SO_2 and NO_2 50-10,000 times faster than previous estimates. Using the results of these direct measurements, they suggest that the reaction of SCI and SO_2 can produce as much SO_4^{2-} as the oxidation of SO_2 by OH. The Comprehensive Air quality model with extensions (CAM_x) and the Community Multiscale Air Quality (CMAQ) are two widely used 3-D models for simulating regional air quality. These models tend to under-estimate SO_4^{2-} compared to observed atmospheric concentrations (Luo et al., 2011). This underestimation can be caused by several reasons including under-estimation of emissions, misrepresentation of meteorological fields, or inadequate chemical production in the atmosphere. Here, we examine the potential impacts of the aqueous-phase oxidation of S(IV) by NO_2 and the gas-phase oxidation of SO_2 by SCI on SO_4^{2-} using the CMAQ model.

2. Methodology

2.1 Model framework

This study uses the Community Multiscale Air Quality (CMAQ) modeling system (version 5.0) (Binkowski and Roselle, 2003; Byun and Schere, 2006). CMAQ is a 3-D, multi-scale, multipollutant chemical transport model that simulates the spatiotemporal evolution of pollutant concentrations over a given modeling domain. It incorporates state-of-the-science representations of the major processes that influence the transformation and transport of airborne chemicals, including advection, diffusion, aerosol dynamics, deposition, processing by clouds, and chemistry (Byun and Schere, 2006). Evaluations of the CMAQ modeling system against ambient measurements have shown that the CMAQ model has considerable skill in simulating O_3 and fine particulate concentrations (Eder and Yu, 2006; Appel et al., 2007; Foley et al., 2010). The modeling domain covers Canada, United States, and Mexico and consists of 299 x 459 horizontal grid-cells with a 12-km horizontal grid-resolution. The model vertical extent is resolved using 35 vertical layers of unequal spacings with a surface layer height of 20-meters. Model simulations were performed for a winter (January) and summer (July) month in 2006. Boundary conditions were generated from GEOS-CHEM model results (Bey et al., 2001). The predefined clean air vertical profiles provided with the CMAQ modeling system were used to set initial conditions. To minimize the impact of initial conditions on predicted results, each model simulation included a ten day spin-up period. Meteorological fields were obtained from the Weather Research and Forecasting model (version 3.3) (Skamarock et al., 2008). The 2005 National Emissions Inventory (http://www.epa.gov/ttn/chief/ net/2005_nei_point.pdf) was used to generate model-ready emissions using the Sparse Matrix Operator Kernel Emissions (SMOKE) model (Houyoux et al., 2000). The Biogenic Emissions Inventory System (version 3.14) was used to prepare biogenic emissions for the study (Schwede et al., 2005). The study uses the updated 2005 Carbon Bond (CB05TU) chemical mechanism (Yarwood et al., 2005; Whitten et al., 2010) which contains the gas-phase chemical reaction of SO_2 and OH. The rate constant of the

reaction is taken from the 2006 NASA/JPL recommendation which is consistent with the value used in the SAPRC07 mechanism (Carter, 2010).

2.2 Aqueous-phase processing of sulfur in CMAQv5.0

CMAQ's aqueous-phase chemistry module is based on that from the Regional Acid Deposition Model (RADM) and includes five sulfur oxidation reactions (Chang et al., 1987; Walcek and Taylor, 1986) with two additional reactions for secondary organic aerosol (Carlton et al., 2010). It contains the following aqueous-phase pathways for the oxidation of S(IV) to SO_4^{2-} (Table 1): (1) H_2O_2, (2) O_3, (3) MHP, (4) PAA, and (5) oxygen catalyzed by iron (Fe[III]) and manganese (Mn[II]).

In previous versions of the CMAQ model, SO_4^{2-} production via R7 was calculated using the prescribed background concentrations of 0.01 $\mu g/m^3$ for Fe(III) and 0.005 $\mu g/m^3$ for Mn(II). As CMAQv5.0 now includes explicit treatment of Fe and Mn aerosol, their tracked concentrations are now used to estimate Fe(III) and Mn(II) values for the metal catalyzed oxidation pathway. To estimate aqueous-phase Fe(III) and Mn(II) concentrations from total (activated) aerosol iron and manganese, the solubility and oxidation state of these species are needed. Iron solubility and oxidation state is highly variable and dependent on a number of factors including origin of the aerosol and time of day, with more soluble iron aerosol found in anthropogenic source regions compared to those areas with high levels of natural dust emissions (Alexander et al., 2009; Seifert et al., 1998). Manganese is typically more soluble than iron and exists mainly as Mn(II) in cloud/fog droplets; whereas iron cycles diurnally, and exists mainly as Fe(II) during the day and Fe(III) at night (Alexander et al., 2009). In CMAQv5.0, the solubility of iron and manganese is kept constant at 10% and 50%, respectively (Alexander et al., 2009). All dissolved manganese is assumed to be Mn(II), and Fe(III) is assumed to be 90% of the dissolved Fe at night and 10% during the day. Note that while only Fe(III) and Mn(II) impact the S(IV) oxidation rate, all Fe and Mn in the activated droplets is subjected to scavenging/deposition. The production rate of SO_4^{2-} for R7 is calculated following Martin and Goodman (1991) as $750[Mn(II)][S(IV)] + 2600[Fe(III)][S(IV)] + 1.0\times10^{-10}[Fe(III)][Mn(II)][S(IV)]$.

2.3 Aqueous-phase oxidation of S(IV) by NO_2

The aqueous-phase oxidation of S(IV) by NO_2 has been well documented in studies of removing combustion gases (SO_2 and NO_x) produced in power plants using scrubbing technology (Shen and Rochelle, 1998; Dahlan et al., 2006; Barreto et al., 2008; Hu et al., 2010). While there has been some disagreement between studies on the details of the reaction mechanism, lab experiments have shown the reaction is favorable under high pH conditions (Lee and Schwartz, 1983; Clifton et al., 1988; Littlejohn et al., 1993) and in the presence of oxygen (Littlejohn et al., 1993; Shen and Rochelle, 1998).

Lee and Schwartz (1983) studied the products and stoichiometry of this reaction by bubbling NO_2 through a HSO_3^- solution and suggested the overall reaction is mainly:

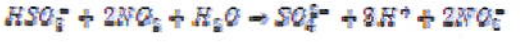

(R8)

with a pH-dependent rate constant (k_8). At pH = 5.0, k_8=1.4×10^5 M^{-1} s^{-1}, but at pH = 5.8 and pH = 6.4 only a low limit of 2×10^6 M^{-1} s^{-1} could be determined. Production rate of SO_4^{2-} is estimated as k_8[S(IV)][NO_2].

Some studies proposed that such a reaction was likely to involve electron transfer that might initiate sulfite oxidation in a chain mechanism (Nash, 1979; Littlejohn, et al., 1993; Shen and Rochelle, 1998, Tursic et al., 2001). The reactions and corresponding rate constants could then be expressed as (Takeuchi et al., 1977):

$$SO_3^{2-} + NO_2 \rightarrow SO_3^{\bullet-} + k_9 = 6.6\times10^8\ M^{-1}s^{-1} \quad \text{(R9)}$$

$$HSO_3^- + NO_2 \rightarrow HSO_3^{\bullet} + k_{10} = 1.3\times10^6\ M^{-1}s^{-1} \quad \text{(R10)}$$

Xue et al. (2012) adopted R9 and R10 and derived an overall reaction rate constant for (R8) of ~1.7×10^5 M^{-1} s^{-1} at pH = 4, 3.0×10^5 M^{-1} s^{-1} at pH = 4.6, and ~2.4×10^6 M^{-1} s^{-1} at pH=6 by solving a series of equations that describe detailed reaction mechanism for the S(IV) + NO_2 (aq) pathway. However, Clifton et al. (1988) argued that the reaction could not take place by a simple electron transfer. They suggested the initial step involves the formation of an additive complex which can undergo subsequent reaction with further dissolved NO_2. The measured rate constants are 1-2 orders of magnitude larger than previous suggested values and are shown in Table 2. The reaction is first order in NO_2 (Clifton et al., 1988; Littlejohn et al., 1993).

Henry's Law coefficients may be used to estimate the relative amount of oxidants dissolved in liquid cloud water. Henry's Law coefficients for five oxidants are shown in Table 3. The Henry's Law coefficient for H_2O_2 is the highest among these, and the Henry's Law coefficients for O_3 and NO_2 are similar though a few orders of magnitude lower than those for H_2O_2, PAA, and MHP. Henry's Law coefficients increase as temperature decreases. Thus, a lower temperature promotes partitioning of more oxidants into liquid cloud water. Consequently, during cool periods when SO_4^{2-} production from oxidants such as H_2O_2 and O_3 is low, the dissolution of NO_2 in cloud droplets in NO_x rich environments could produce a pathway for conversion of S(IV) to SO_4^{2-}.

2.4 Gas-phase oxidation of SO_2 by SCI

The CB05TU mechanism used does not include SCI chemistry so modifications are needed to explicitly represent the SCI and its subsequent chemical reactions. Although the model simulations in this study use the CB05TU mechanism, the modifications made to CB05TU to represent SCI reactions are based on the more detailed SAPRC07 mechanism (Carter, 2010). The calculation of SCI yields is more straightforward for SAPRC07 because the reactions of the lumped species can be related back to the detailed mechanisms for the individual compounds they represent (Carter, 2010), and the SCI yields for the various compounds have been measured or can be estimated. This is not the case for the CB05TU mechanism, where other methods are used to derive the mechanisms for the lumped model species. Examples of SCI yields for various compounds are summarized in Table 4.

In most cases, the SCI yields for the individual compounds in the detailed SAPRC07 mechanism can be equated directly to the organic acid yields in the O_3 + alkene reactions, because SAPRC07 assumes that the SCI species react

with H_2O to form the corresponding acid. Thus, acid model species are used to represent the SCI formation. The only exception concerns some of the terpenes whose mechanisms are used to derive that for the terpene (TERP) model species, where some of the organic acids formed from the SCI + H_2O reaction also contain carbonyl groups, and are represented by the PROD2 model species. In those cases, the details of the mechanisms were examined to derive the appropriate SCI yield for these model species.

Whitten et al. (2010) describe the CB05TU mechanism; here only the changes made to represent the explicit SCI and subsequent chemistry are discussed. Table 5 lists the modifications made to the CB05TU mechanism to represent the effects of SCI formation on sulfate and NO_3 formation. The model species "CRIEGEE" was added to the mechanism to represent SCI formation, and its reactions are included in Table 5. The SCI yields for the reactions of O_3 with the CB05TU model species were derived by assuming the yields derived for the lumped species in SAPRC07 that represents the most similar set of compounds. Other than the addition of the CRIEGEE model species the reaction products and rate constants as described by Yarwood et al. (2005) and Whitten et al. (2010) are not changed.

The CB05TU mechanism contains 172 reactions; three additional reactions are added to the mechanism (173-175) to describe the chemical sinks for CRIEGEE model species. SCI reacts with SO_2, NO_2, H_2O and NO (Welz et al., 2012). However, the reaction rate with NO is low; thus the consumption of CRIEGEE via the NO reaction is neglected for any further consideration. The reaction of CRIEGEE with SO_2 produces SULF while the reaction with NO_2 produces NO_3 radical. Note that this representation does not include the effect of the different SCI reactions on formation of organic products, which are assumed to be unchanged regardless of how SCI reacts. For this reason, the reaction of CRIEGEE with H_2O, which affects only organic product formation, only represents the consumption of CRIEGEE by this process, and thus has no product formation. The standard mechanism is based on the assumption that most of the SCI reacts with H_2O, and the changes in organic product formation resulting with the SCI reaction with SO_2 or NO_2 is not represented. However, the representation of organic products in CB05TU is highly condensed, so changes in product model species yields may not be indicated. In any case, this approximate and lumped representation is sufficient to represent the effect of the SCI reactions on sulfur chemistry, which is the primary objective of this study.

Absolute rate constants for the reactions of CRIEGEE with SO_2 and NO_2 are based on the recent direct measurements of Welz et al. (2012). The critical parameter is the rate constant ratio of the reactions of SCI with H_2O and SO_2. Welz et al., (2012) provided only an upper limit of 4.0×10^{-15} cm^3 $molecule^{-1}s^{-1}$ for the reaction of SCI with H_2O which translates to a value of $<1.0 \times 10^{-4}$ for the rate constant ratio of the reactions of SCI with H_2O and SO_2. While several studies provided rate constants for the reaction of SCI and H_2O, the amount of useful information is quite limited. There seem to be no quantitative measurements of the absolute rate constant. Hatakeyama and Akimoto (1994) conducted a review of the SCI and suggested a rate constant for the reaction of SCI and H_2O based

on a relative rate constant. Since the absolute rate constant for the reaction of SCI with SO_2 is higher than previously believed, the rate constant for the reaction of SCI with H_2O based on relative rate measurements will also be higher. Calvert et al. (2000) compiled rate constant ratios for the reactions of SCI with H_2O and SO_2 ranging from 6.1×10^{-5} to 8.3×10^{-4}. The ratios based on the study of Suto et al. (1985), Becker et al. (1990), and Neeb et al. (1998) are higher than the upper limit ratio of 1.0×10^{-4} from Welz et al. (2012) and thus, we do not use these values. The other ratio of 6.1×10^{-5} is from Calvert et al. (1978) and about half of the upper limit suggested by Welz et al. (2012). Since there is not any other known measurement, and this is consistent with the upper limit of Welz et al. (2012), the rate constant for the SCI and H_2O adopted here follows Calvert et al. (1978).

2.5 Simulation details

Four different simulations were completed (Table 6) for January and July 2006. The first simulation used the CB05TU chemical mechanism and the default aqueous-phase chemical reactions in CMAQv5.0. The second simulation used the CB05TU chemical mechanism, the default aqueous-phase chemical reactions, and the aqueous-phase oxidation of S(IV) by NO_2 with the lower rate constant reported by Lee and Schwartz (1983). The model used interpolated values between pH 5.0 and 6.0. For cloud water pH below 5.0, the model used 1.4×10^5 $M^{-1}s^{-1}$ and for cloud water pH above 6.0, the model used 2.0×10^6 $M^{-1}s^{-1}$. The third simulation was similar to the second simulation except that the aqueous-phase oxidation of S(IV) by NO_2 with the higher rate constant reported by Clifton et al. (1988) was used. We fitted an equation (Figure 1) using the reported rate constants at different pH and used it to calculate the rate constant. For cloud water pH below 5.3, the minimum value reported by Clifton et al. (1988) was used. Differences in the results between the third or the second and first simulations are attributed to the aqueous-phase oxidation of S(IV) by NO_2. The fourth simulation used the CB05TU chemical mechanism augmented by the SCI chemistry and the default aqueous-phase chemical reactions in CMAQv5.0. Differences in the results between the fourth and the first simulations are attributed to the gas-phase SO_2 oxidation by the SCI.

3. Results and discussions

3.1 Impact of the aqueous-phase oxidation of S(IV) by NO_2 on SO_4^{2-}

Changes between predicted mean wintertime SO_4^{2-}, SO_2, and NO_2 with and without the aqueous-phase oxidation of S(IV) by NO_2 (with the higher rate constant) are shown in Figure 2. Mean SO_4^{2-} levels reach more than 2.5 $\mu g/m^3$ in most areas of the eastern US while values are less than 1.0 $\mu g/m^3$ for the western US. The aqueous-phase oxidation of S(IV) by NO_2 enhances the monthly mean SO_4^{2-} by 12-20% in the midwest and northeastern US and 4-12% over other areas of the eastern US. Although not shown here, it also enhances SO_4^{2-} aloft. Mean SO_2 levels exceed 15 $\mu g/m^3$ in the Ohio Valley region while mean NO_2 levels exceed 16.0 ppbv in many urban areas. The reaction consumes SO_2 and NO_2 thereby decreasing their levels. Mean SO_2 decreases by 0.6-3.0% while mean NO_2 decreases by 1.0-5.0%. It enhances SO_4^{2-} in areas with elevated NO_2 and SO_2. The aqueous-phase oxidation of S(IV) by NO_2 with the lower rate constant also enhances mean wintertime SO_4^{2-} by 0.4-1.2% in the northeastern US (not shown). Thus, the reaction with the lower or higher rate constant leads to increases in wintertime SO_4^{2-}.

295 Changes between predicted mean wintertime nitrate, ammonium, and O_3 with and without the aqueous-phase
296 oxidation of S(IV) by NO_2 (with the higher rate constant) are shown in Figure 3. Mean nitrate levels reach 4.0 $\mu g/m^3$
297 in the Midwest, northeastern US, and central California while lower values exist in other areas. The reaction
298 decreases mean nitrate by 2-10% over a large area of the eastern US. Sulfuric acid has a very low vapor pressure and
299 tends to reside primarily in the aerosol phase. In a system of sulfuric acid, water, ammonia, and nitric acid, available
300 ammonia preferentially reacts with sulfuric acid and only excess ammonia is available to form NH_4NO_3 (Seinfeld
301 and Pandis, 2006). Since the aqueous-phase oxidation of S(IV) by NO_2 increases sulfate, less ammonia is available
302 to form NH_4NO_3 and thus higher $HNO_3(g)$ and lower $NH_3(g)$ levels may be expected with the addition of the S(IV)
303 + NO_2 reaction. Mean ammonium levels reach more than 2.5 $\mu g/m^3$ in most areas of the eastern US and central
304 California. The S(IV) oxidation by NO_2 enhances mean ammonium by 0.4-2.0%. By increasing sulfate, the reaction
305 leads to a net increase in ammonium levels (i.e., the ammonium associated with increased sulfate exceeds the
306 amount lost to the decreased nitrate levels). Mean O_3 concentrations reach more than 20 ppbv in most areas of the
307 US. Higher values are predicted in the western US than those in the eastern US. The reaction enhances mean O_3
308 only by 0.2-1.0% due to changes in NO_2.
309
310 Changes between predicted mean summertime SO_4^{2-} with and without the aqueous-phase oxidation of S(IV) by NO_2
311 (with the higher rate constant) are shown in Figure 4. Predicted mean summertime SO_4^{2-} levels exceed 5.0 $\mu g/m^3$
312 over a large portion of the eastern US while values are less than 1.0 $\mu g/m^3$ for most of the western US. The impact
313 of the aqueous-phase oxidation of S(IV) by NO_2 on SO_4^{2-} is negligible in most areas. It only enhances the monthly
314 mean SO_4^{2-} in isolated grid-cells by 0.4-2.0%. The impact of the aqueous-phase oxidation of S(IV) by NO_2 with the
315 lower rate constant on summertime SO_4^{2-} is even smaller. Oxidant levels in summer are much higher than those in
316 winter due to higher temperature and actinic flux. Summertime SO_4^{2-} production is typically dominated by aqueous-
317 phase production via the H_2O_2 pathway and the gas-phase reaction of SO_2 with OH (Seigneur and Saxena, 1988;
318 Mathur et al., 2008). Since wintertime H_2O_2 and OH are lower, the wintertime production via these pathways is also
319 lower. Winter SO_2 and NO_2 levels are generally higher than those in summer in the US (Figure 9). The lower
320 temperature helps partitioning more SO_2 and NO_2 into cloud water and enhance the production of SO_4^{2-} via the
321 aqueous-phase oxidation of S(IV) by NO_2 in winter. Thus, the production of SO_4^{2-} via the aqueous-phase oxidation
322 of S(IV) by NO_2 can effectively compete with these pathways and affect SO_4^{2-} levels in winter but not in summer.
323
324 **3.2 Day-to-day variation of the enhanced SO_4^{2-} due to the aqueous-phase oxidation of S(IV) by NO_2**
325 Here we examine the day-to-day variation of the changes in wintertime SO_4^{2-} due to the aqueous-phase oxidation of
326 S(IV) by NO_2. The aqueous-phase oxidation of S(IV) by NO_2 affected sulfate in the Midwest by a relatively high
327 percentage (Figure 2). Time series of daily-averaged SO_4^{2-} without the aqueous-phase oxidation of S(IV) by NO_2 are
328 plotted along with changes due to the aqueous-phase oxidation of S(IV) by NO_2 for a representative grid-cell in the
329 Midwest in Figure 5. Predicted SO_4^{2-} without the additional NO_2 oxidation pathway range between 1.0-3.0 $\mu g/m^3$
330 except on two days. Predicted SO_4^{2-} on January 2 reaches 5.0 $\mu g/m^3$, and on January 25, it drops to 0.5 $\mu g/m^3$. The
331 aqueous-phase oxidation of S(IV) by NO_2 does not increase SO_4^{2-} on all days, but it does increase SO_4^{2-} on many

days including three days when the reaction increases SO_4^{2-} by almost 100%. The impact on SO_4^{2-} on other days is smaller. Similar day-to-day variations are observed in other areas.

3.3 Impact of the gas-phase oxidation of SO_2 by SCI on SO_4^{2-}

The maximum predicted SCI concentrations in winter and summer are shown in Figure 6. Higher values in summer are predicted in the western and southeastern US while lower values are predicted in other areas. Predicted values in summer are greater than those in winter due to higher alkene emissions and reaction rates. Predicted summertime values are slightly lower than the "low" value of 4.5×10^4 molecules cm^{-3} suggested by Welz et al., (2012). However, the "low" value suggested by Welz et al., (2012) represents episodic levels of localized polluted environments. In this study, we simulated the entire continental US using relatively large horizontal grid-sizes and by using the best available emissions estimates. Consequently, values represent an average over the large volume in a grid-cell and hence lower values are expected.

Changes in mean SO_4^{2-} due to the SCI chemistry are shown in Figure 7. The SCI chemistry enhances the monthly mean wintertime SO_4^{2-} only by 0.4-1.2% over a small area in the northeast US and does not enhance SO_4^{2-} in most areas in the summer. It only enhances SO_4^{2-} by 1.2-2.0% over a small area in Montana. It should be noted that predicted SO_4^{2-} concentrations without the SCI chemistry in Montana are small; the SCI chemistry only marginally increases SO_4^{2-}. For typical atmospheric conditions of SO_2 = 10 ppbv, NO_2= 10 ppbv, H_2O = 10,000 ppmv (T = 25 ^{0}C, RH = 35%), we calculate that the reaction of SCI and H_2O accounts for more than 95% of the total consumption rate of SCI. Thus, the impact of the oxidation of SO_2 by SCI on SO_4^{2-} is negligible.

3.4 Sensitivity of the predicted SO_4^{2-} due to the gas-phase oxidation of SO_2 by SCI

Here, we examine the sensitivity of predicted SO_4^{2-} to the rate constant for the SCI reaction of with H_2O. Welz et al. (2012) reported an upper limit of 4.0×10^{-15} cm^3 $molecule^{-1}$ s^{-1} for the rate constant. However, based on an assumed value of 1.0×10^{-16} cm^3 $molecule^{-1}$ s^{-1} (40 times lower than the upper limit), they suggested the SCI chemistry can enhance atmospheric SO_4^{2-} by as much as the oxidation of SO_2 by OH. We conducted another simulation for a 10-day period in July (July 1-10) using the lower rate constant of 1.0×10^{-16} cm^3 $molecule^{-1}$ s^{-1} for the reaction of SCI and H_2O. Predicted mean SO_4^{2-} without SCI chemistry and increases in mean SO_4^{2-} due to SCI chemistry for the two alternate SCI+H_2O rate constants are shown in Figure 8. Predicted mean SO_4^{2-} levels exceed 4.0 $\mu g/m^3$ in the Southeast and Midwest while values are less than 1.0 $\mu g/m^3$ for most of the western US. As indicated earlier, the SCI chemistry with the higher rate constant for the SCI and H_2O reaction does not enhance SO_4^{2-}. However, the SCI chemistry with the lower rate constant for this reaction enhances SO_4^{2-} by 2.0-10.0% over a large area in both the eastern and western US. Consequently the relative importance of the SCI mediated SO_4^{2-} production pathway is dependent also on accurately characterizing atmospheric SCI chemical sinks.

3.5 Comparison of model predictions with observed data

Time series of the predicted NO_2 concentrations with and without the aqueous-phase reaction of S(IV) and NO_2 are compared to observations from the USEPA's Air Quality System in Figure 9. Observed wintertime NO_2 values range between 8-18 ppbv while summer values range between 6-12 ppbv. Summertime concentrations are lower than winter values due to higher boundary layers and greater atmospheric oxidation capacity. Predicted NO_2 concentrations in winter compare well with the observed data. This suggests the production of wintertime SO_4^{2-} via the aqueous-phase oxidation of S(IV) by NO_2 is not due to any unusually high NO_2 values used in the model. Predicted summertime NO_2 values are greater than the observed concentrations by ~50% due primarily to the high nighttime predictions. Despite the higher NO_2 values in the model, the aqueous-phase reaction of S(IV) and NO_2 does not enhance summertime SO_4^{2-}.

The median and inter-quartile range of observed SO_4^{2-} from the Clean Air Status and Trends Network (CASTNet) sites are shown in Figure 10(a-b). It should be noted that CASTNet data are weekly averaged and data from all monitoring sites are used to compute the values shown in the figure. Predicted values with and without the aqueous-phase reaction of S(IV) and NO_2 are also shown in the figure. Observed SO_4^{2-} levels are greater than those predicted both in winter and summer. However, due to the increased sulfate from the aqueous-phase reaction of S(IV) and NO_2, the reaction leads to improved model performance for winter SO_4^{2-}. It does not affect the comparison of model predictions in summer. Additional SO_4^{2-} production is needed to further improve model predictions in winter as well as in summer. Since the impact of the SCI chemistry on SO_4^{2-} is negligible, predicted SO_4^{2-} concentrations are not compared to the observed data.

4. Summary and conclusions

We examined the impact of the aqueous-phase oxidation of S(IV) by NO_2 and the gas-phase oxidation of SO_2 by SCI on SO_4^{2-} using the Community Multiscale Air Quality modeling system. To our knowledge, this is the first study that employs both of these reactions for assessing the importance of these pathways relative to the conventional SO_2 oxidation pathways. Our results suggest that the relative importance of aqueous-phase oxidation of S(IV) by NO_2 shows distinct seasonal trends by enhancing SO_4^{2-} in the winter but not in summer. Consistent with the conventional view of sulfur chemistry, summertime conversion of SO_2 into SO_4^{2-} is dominated by the aqueous-phase oxidation by H_2O_2 and gas-phase oxidation by OH. Atmospheric levels of H_2O_2 and OH in winter are lower than those in summer; consequently, the wintertime conversion of SO_2 to SO_4^{2-} via these pathways is also lower. Thus, the aqueous-phase oxidation of S(IV) by NO_2 can compete more effectively with these pathways to enhance SO_4^{2-} production in the winter. Pandis and Seinfeld (1989) studied acid deposition for a winter episode in 1985 and suggested that the reaction contributes considerably to the sulfate production in San Joaquin Valley of California. Our results over a larger geographic domain and for much lower SO_2 and NO_x levels in the current atmosphere are similar to the findings of Pandis and Seinfeld (1989) on the relative importance of this pathway.

We find the gas-phase oxidation of SO_2 by SCI does not affect SO_4^{2-} appreciably. Our regional scale calculations do not show the large and widespread increase that may be inferred from the results of Welz et al. (2012) who

suggested that the pathway can enhance SO_4^{2-} by as much as the oxidation of SO_2 by OH. The disagreement arises due to the chosen value for the rate constant of the reaction of SCI and H_2O. We use a value which is two times lower than the upper limit of 4.0×10^{-15} cm^3 $molecule^{-1}$ s^{-1} measured by Welz et al. (2012) but 24 times greater than the value of 1.0×10^{-16} cm^3 $molecule^{-1}$ s^{-1} which they used for their analysis of the potential atmospheric impacts of the SCI + SO_2 reaction. In our study, the majority of the SCI is consumed by the reaction of SCI and H_2O; consequently, the additional SCI chemistry does not significantly enhance SO_4^{2-}. Consistent with the results of Welz et al. (2012), the use of the lower rate constant, however, can potentially enhance SO_4^{2-} concentrations.

These results suggest that the rate constants of the aqueous-phase reaction of S(IV) and NO_2 and the gas-phase reaction of SCI and H_2O are important and should be further examined. We hope this study will motivate the atmospheric chemistry community to further study these reactions to improve our current understanding of sulfur chemistry.

Disclaimer

Although this paper has been reviewed by EPA and approved for publication, it does not necessarily reflect EPA's policies or views.

References

Alexander, B., Park, R.J., Jacob, D.J., Gong, S., 2009. Transition metal-catalyzed oxidation of atmospheric sulfur: global implications for the sulfur budget, Journal of Geophysical Research, 114, D02309.

Appel, K. W., Gilliland, A. B., Sarwar, G., and Gilliam, R. C.: Evaluation of the Community Multiscale Air Quality (CMAQ) model version 4.5: Sensitivities impacting model performance, Part I-Ozone, Atmos. Environ., 41, 9603–9615, 2007.

Barreto, A. E. H., Correa, M.M., Munoz, A.O., and de Correa, C.M., 2008. Cement plant gaseous pollutant emission reduction technologies, Revista Ingenieria E Investigacion 28, 41-46.

Bey, I., Jacob, D. J., Yantosca, R. M., Logan, J. A., Field, B. D., Fiore, A. M., Li, Q., Liu, H. Y., Mickley, L. J., and Schultz, M. G., 2001: Global modeling of tropospheric chemistry with assimilated meteorology: Model description and evaluation, J. Geophys. Res., 106, 23073–23096.

Becker, K.H., Brockmann, K.J., and Bechara, J., 1990: Production of hydrogen peroxide in forest air by reaction of ozone with terpenes, Nature, 346, 256-258.

Binkowski, F. S. and Roselle, S. J.: Community Multiscale Air Quality (CMAQ) model aerosol component, I: Model description, J. Geophys. Res., 108, 4183, doi:10.1029/2001JD001409, 2003.

Byun, D. and Schere, K. L., 2006. Review of the governing equations, computational algorithms, and other components of the Models-3 Community Multiscale Air Quality (CMAQ) Modeling System, Applied Mechanics Reviews 59, 51-77.

Calvert, J. G., Su, F., Bottenheim, J.W., and Strausz, O.P.; 1978. Mechanism of the homogeneous oxidation of sulfur dioxide in the troposphere, Atmospheric Environment 12, 197-226.

Calvert, J. G., Stockwell, W.R., 1983. Acid generation in the trophosphere by gas-phase chemistry, Environmental Science & Technology, 17, 428A-443A.

Calvert, J. G., Atkinson, R., Kerr, J.A., Madronich, S., Moortgat, G.K., Wallington T.J., Yarwood, G.: The mechanism of the atmospheric oxidation of the alkenes, Oxford University Press, New York, USA, 2000.

Carlton, A. G., Bhave, P. V., Napelenok, S. L., Edney, E. O., Sarwar, G., Pinder, R. W., Pouliot, G. A., M. Houyoux, 2010. Model representation of secondary organic aerosol in CMAQv4.7, Environmental Science and Technology, 44, 8553–8560.

Carter, W.P.L., 2010. Development of the SAPRC-07 chemical mechanism, Atmospheric Environment 44, 5336-5345.

Chang, J. S., Brost, R. A., Isaksen, I. S. A., Madronich, S., Middleton, P., Stockwell, W. R., and C. J. Walcek, 1987. A three-dimensional Eulerian acid deposition model: physical concepts and formulation, Journal of Geophysical Research, 92 (D12), 14681-14700.

Clifton, C. L., Altstein, N. and Huie, RE., 1988. Rate constant for the reaction of NO2 with sulfur(IV) over the pH range 5.3-13, Environmental Science & Technology, 22, 586-589.

Cox, R.A. and Penkett, S.A., 1971. Oxidation of atmospheric SO_2 by the products of the ozone-olefin reaction, Science, 230, 321-322, 1971.

Cox, R.A. and Penkett, S.A., 1972. Aerosol formation from sulphur dioxide in the presence of ozone and olefinic hydrocarbons, Journal of the Chemical Society, Faraday Transactions 1., 68, 1735-1753.

Chameides, W., 1984. The photochemistry of a remote marine stratiform cloud, J. Geophys. Res., 89, 4739-4755.

Dahlan, I., Lee K.T., Kamaruddin, A.H, and Mohamed, AR, 2006. Key factor in rice husk ash/CaO sorbent for high flue gas desulfurization activity, Environmental Science & Technology, 40, 6032-6037.

Eder, B. and S. Yu, 2006: A performance evaluation of the 2004 release of Models-3 CMAQ. *Atmos. Environ.*, 40, 4811-4824.

Finlayson-Pitts, B. J. and Pitts Jr., J. N.: Chemistry of the Upper Lower Atmosphere, Theory, Experiments and Applications, Academic Press, San Diego, 2000.

Foley, K. M., Roselle, SJ., Appel, K.W., Bhave, P.V., Pleim, JE., Otte, T. L., Mathur, R., Sarwar, G., Young, J.O., Gilliam, R.C., Nolte, C.G., Kelly, J.T., Gilliland, A.B., and Bash, JO., 2010. Incremental testing of the Community Multiscale Air Quality (CMAQ) modeling system version 4.7, Geosci. Model Dev., 3, 205–226.

Hasson, A.S., Ho, A.W, Kuwata, KT., Paulson, S.E., 2001. Production of stabilized Criegee intermediates and peroxides in the gas phase ozonolysis of alkenes 2. Asymmetric and biogenic alkenes, Journal of Geophysical Research, 106, D24, 34,143-34,153.

Hatakeyama, S., Akimoto, H., 1994. Reactions of Criegee intermediates in the gas-phase, Research Chemical Intermediates, 20, 503-524.

Houyoux, M. R., Vukovich, J. M., Coats Jr., C. J., Wheeler, N. M., and Kasibhatla, P. S.: Emission inventory development and processing for the seasonal model for regional air quality (SMRAQ) project, J. Geophys. Res., 105, 9079–9090, 2000.

Hu, G. X., Sun, Z. G., and Gao, H. Y., 2010. Novel Process of Simultaneous Removal of SO2 and NO2 by Sodium Humate Solution, Environmental Science & Technology, 44, 6712-6717.

Huie, R.E. and Neta, P., 1986. Kinetics of one-electron transfer reactions involving ClO_2 and NO_2. J. Phys. Chem., 90, 1193-1198.

Jacobson, M., 1997. Development and application of a new air pollution modeling system II. Aerosol module structure and design, Atmospheric Environment, 31, 131-144.

Kosak-Channing, L.F.; Helz, G.R., 1983. Solubility of ozone in aqueous solutions of 0-0.6M ionic strength at 5-30 ^{0}C, Environ. Sci. Technol., 17, 145-149.

Lee, Y. N., and Schwartz, S. E., 1983. Kinetics of oxidation of aqueous sulfur(IV) by nitrogen dioxide, in Precipitation Scavenging, Dry Deposition and Resuspension, Vol.1, H.R. Pruppacher, R. G. Semonin, and W. G. N. Slinn, eds., Elsevier, New York.

Littlejohn, D., Wang, Y. Z., and Chang, S. G., 1993. Oxidation of Aqueous Sulfite Ion by Nitrogen-Dioxide, Environmental Science & Technology, 27, 2162-2167.

Luo, C., Wang, Y., Mueller, S., Knipping, E., 2011. Diagnosis of an underestimation of summertime sulfate using the Community Multiscale Air Quality Model, Atmospheric Environment, 45, 5119-5130.

Martin, R.L. and Good, .W., 1991. Catalyzed oxidation of sulfur dioxide in solution: the iron-manganese synergism, Atmospheric Environment, 25A, 2395-2399.

Mathur, R., Roselle, S., Pouliot, G., and Sarwar, G., 2008. Diagnostic analysis of the three dimensional sulfur distributions over the Eastern United States using the CMAQ model and measurements from the ICARTT field experiment, in: Air pollution modeling and its application. XIX, NATO, Science for Peace and Security Series C: Environmental Security, 5, 496–504, doi:10.1007/978-1-4020-8453-9 54.

Nash, T., 1979. Effect of Nitrogen-Dioxide and of Some Transition-Metals on the Oxidation of Dilute Bisulfite Solutions, Atmospheric Environment, 13, 1149-1154.

Neeb, P., Horie, O., Moortgat, G. K., 1998. The ethene-ozone reaction in the gas-phase, J Chem. Phys. A. 102, 6778-6785.

O'Sullivan, D.W., Lee, M., Noone, B.C., Heikes, B.G., 1996. Henry's law constant determinations for hydrogen peroxide, methyl hydroperoxide, hydroxymethyl hydroperoxide, ethyl hydroperoxide, and peroxyacetic acid, J. Phys. Chem., 100, 3241-3247.

Pandis, S. N., and Seinfeld, JH., 1989, Mathematical-Modeling of Acid Deposition Due to Radiation Fog, Journal of Geophysical Research-Atmospheres, 94, 12911-12923.

Schwede, D., Pouliot, G., and Pierce, T. 2005. Changes to the biogenic emissions inventory system version 3 (BEIS3), 4th Annual CMAS Models-3 Users' Conference, September 26-28, 2005, UNC-Chapel Hill, NC.

Seigneur, C. and Saxena, P., 1988. A theoretical investigation of sulfate formation in clouds, Atmospheric Environment 22, 101–115.

Seifert, R.L., Johansen, A.M., Hoffman, MR., and Pehkonen, SO., 1998. Measurements of trace metal (Fe, Cu, Mn, Cr) oxidation states in fog and stratus clouds, J. Air and Waste Manage. Assoc., 48, 128-143.

Seinfeld, J.H. and Pandis, S.N., 1998. Atmospheric Chemistry and Physics: From Air Pollution to Global Change. Wiley, New York.

Seinfeld, J. H., and Pandis, S. N., 2006. Atmospheric chemistry and Physics, Willey Express.

Shen, C. H., and Rochelle, G. T., 1998. Nitrogen dioxide absorption and sulfite oxidation in aqueous sulfite, Environmental Science & Technology, 32, 1994-2003.

Skamarock, W. C., Klemp, J. B., Dudhia, J., Grill, D. O., Barker, D. M., Duda, M. G, Huang, X-Y, Wang, W., and Powers, J. G., 2008. A description of the advanced research WRF version 3. NCAR Tech Note NCAR/TN 475 STR, 125 pp. [Available from UCAR Communications, P.O. Box 3000, Boulder, CO 80307.]

Suto, M., Manzanares, E.R., Lee, L. C., 1985.Detection of sulfuric acid aerosols by ultraviolet scattering, Environmental Science & Technology, 19, 815–820.

Takeuchi, H., Ando, M., Kizawa, N., 1977. Absorption of nitrogen dioxide in aqueous sodium sulfite and bisulfite solutions, Ind. Eng. Chem. Process Des. Dev, 16, 303-308.

Tursic, J., I. Grgic, and Bizjak, M., 2001. Influence of NO2 and dissolved iron on the S(IV) oxidation in synthetic aqueous solution, Atmospheric Environment, 35, 97-104.

Walcek, C. J. and Taylor, G. R., 1986. A theoretical method for computing vertical distributions of acidity and sulfate production within cumulus clouds, Journal of the Atmospheric Sciences, 43 (4), 339-355.

Welz, O., Savee, J.D., Osborn, D.L., Basu, S.S., Percival, C. J., Shallcross, D.E., Taatjes, C.A., 2012. Direct kinetic measurements of Criegee Intermediate (CH_2OO) formed by reaction of CH_2I with O_2. Science, 335, 204-207.

Whitten, G. Z., Heo, Kimura, G. Y., McDonald-Buller, E., Allen, D., Carter, W.P.L, Yarwood, G., 2010. A new condensed toluene mechanism for Carbon Bond: CB05-TU. *Atmospheric Environment,* 44, 5346-5355.

Xue J., Yu, J. Z., Lau, A. K. H. and Yuan, Z. B., 2012. An observation-based box model for secondary inorganic aerosols, submitted to Atmos. Chem. Phys. Discuss.

Figure 1: Rate constant of the aqueous-phase chemical reaction of S(IV) and NO_2 as a function of pH (Clifton et al., 1988)

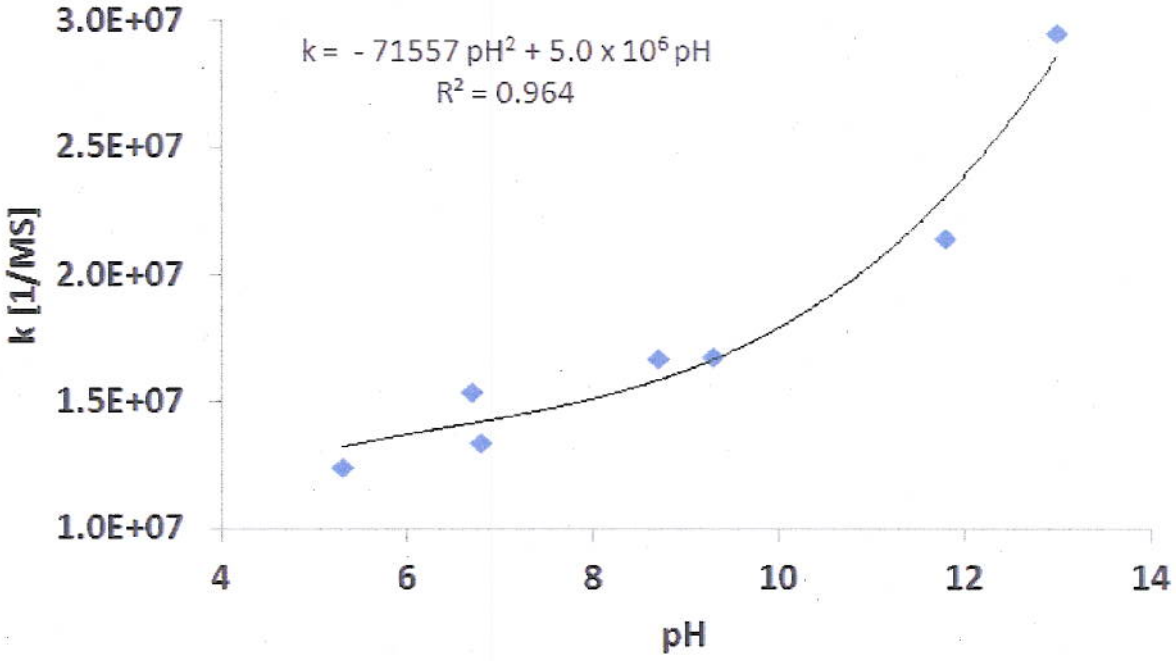

Figure 2: Winter (a) predicted mean sulfate without the aqueous-phase oxidation of S(IV) by NO_2 (b) % difference in mean sulfate due to the aqueous-phase oxidation of S(IV) by NO_2 (higher rate constant) (c) predicted mean SO_2 without the aqueous-phase oxidation of S(IV) by NO_2 (d) % difference in mean SO_2 due to the aqueous-phase oxidation of S(IV) by NO_2 (higher rate constant) (e) predicted mean NO_2 without the aqueous-phase oxidation of S(IV) by NO_2 (f) % difference in mean NO_2 due to the aqueous-phase oxidation of S(IV) by NO_2 (higher rate constant)

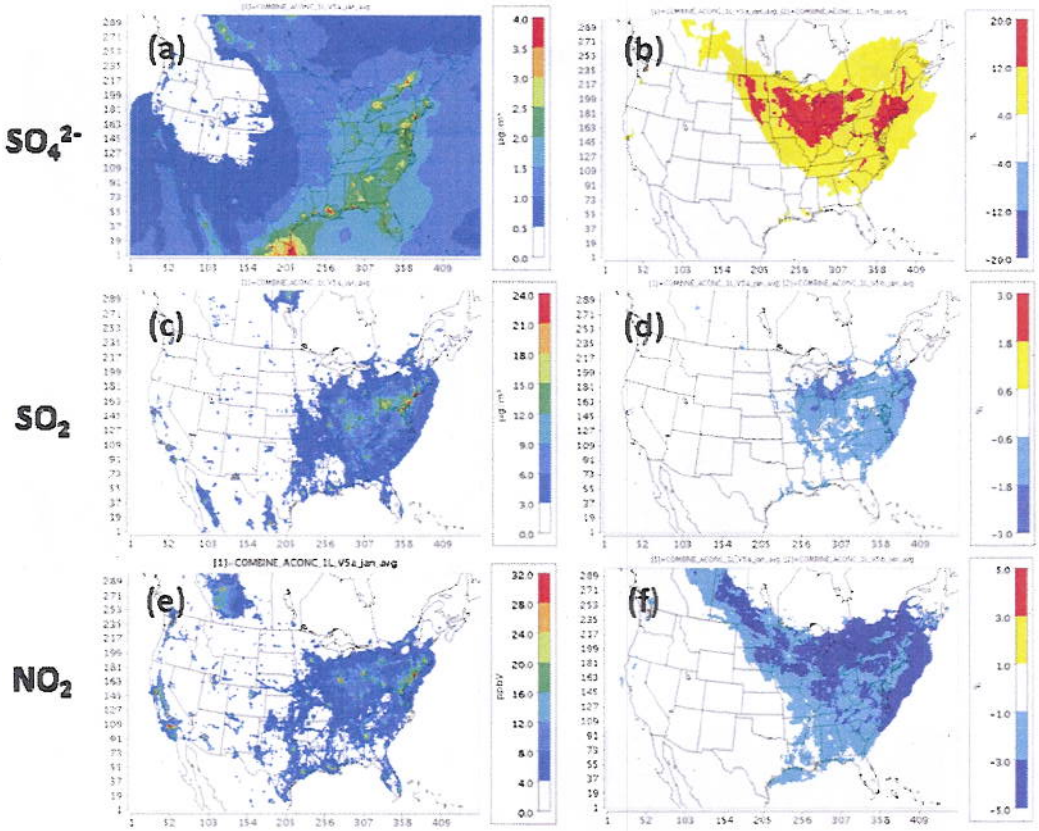

Figure 3: Winter: (a) predicted mean nitrate without the aqueous-phase oxidation of S(IV) by NO_2 (b) % changes in mean nitrate due to the aqueous-phase oxidation of S(IV) by NO_2 (higher rate constant) (c) predicted mean ammonium without the aqueous-phase oxidation of S(IV) by NO_2 (d) % changes in mean ammonium due to the aqueous-phase oxidation of S(IV) by NO_2 (higher rate constant) (e) predicted mean ozone without the aqueous-phase oxidation of S(IV) by NO_2 (f) % changes in mean ozone due to the aqueous-phase oxidation of S(IV) by NO_2 (higher rate constant)

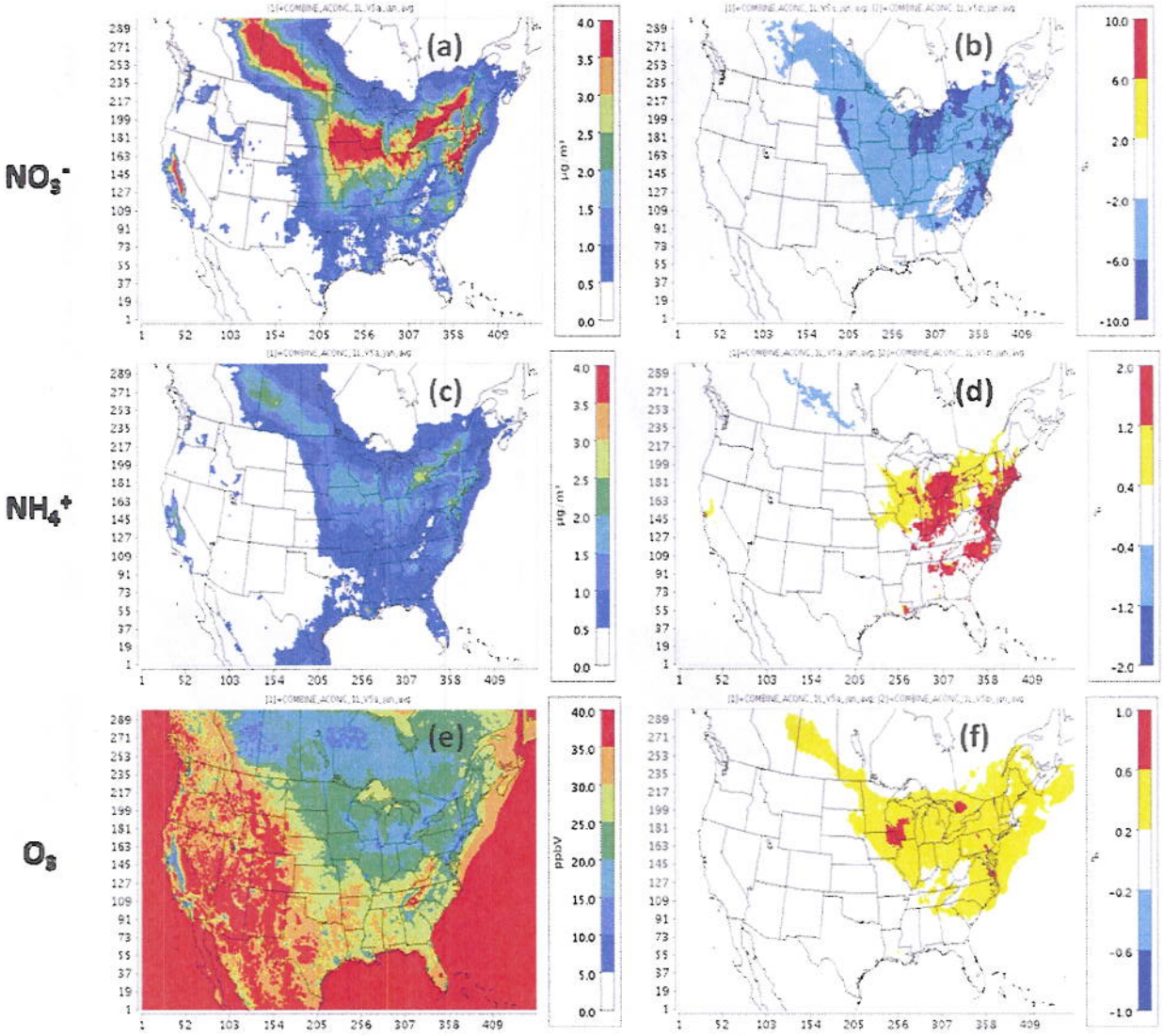

Figure 4: Summer: (a) predicted mean sulfate without the aqueous-phase oxidation of S(IV) by NO_2 (b) % changes in mean sulfate due to the aqueous-phase oxidation of S(IV) by NO_2 (higher rate constant)

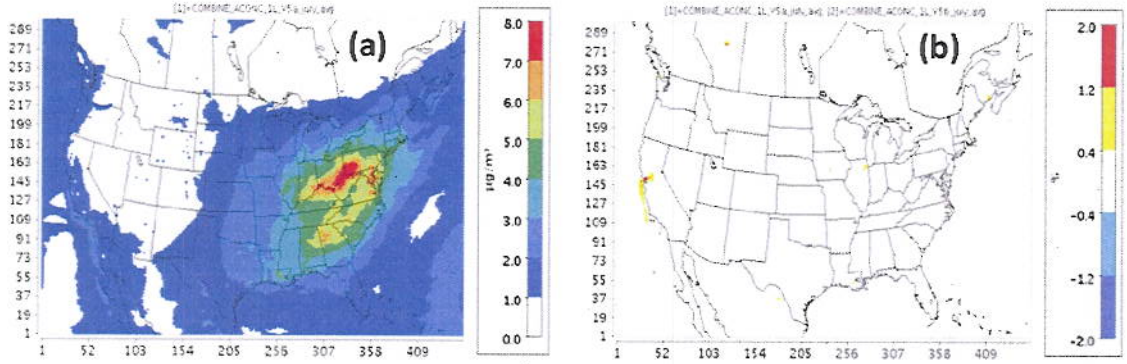

Figure 5: Winter: day-to-day variation of daily-averaged sulfate without the aqueous-phase oxidation of S(IV) by NO_2 and changes in daily-averaged sulfate due to the aqueous-phase oxidation of S(IV) by NO_2 (higher rate constant) for a grid-cell in the Midwest

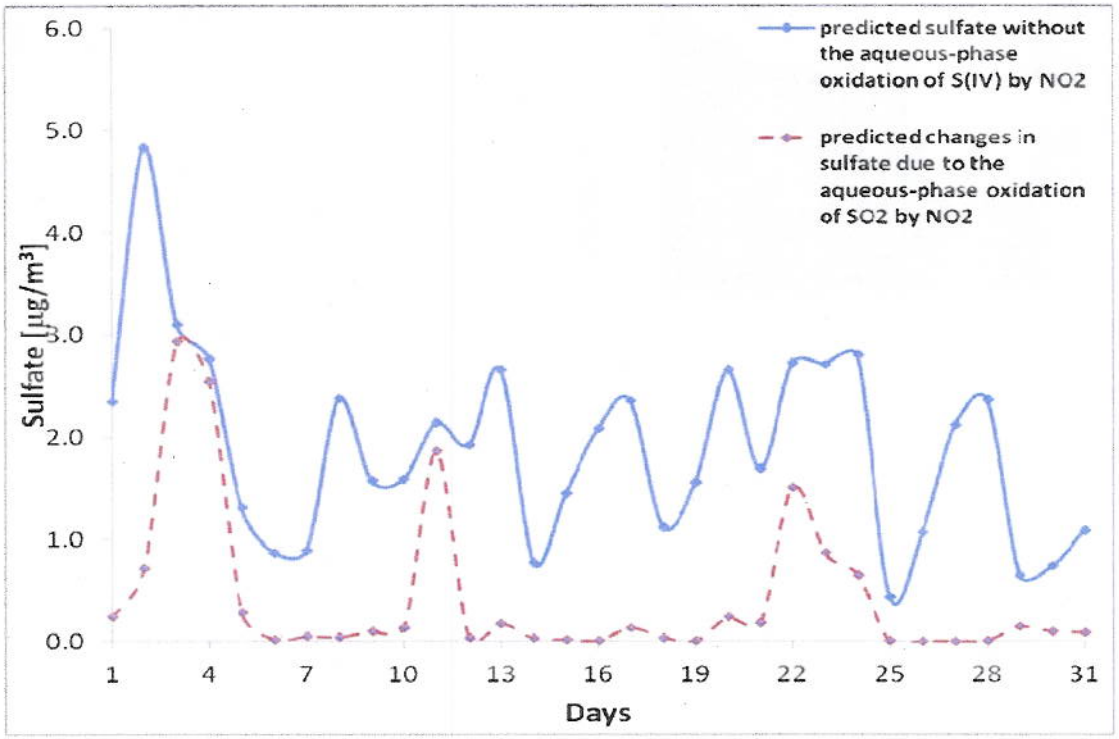

Figure 6: Predicted maximum Stablized Criegee Intermediate (SCI) concentrations in (a) winter and (b) summer

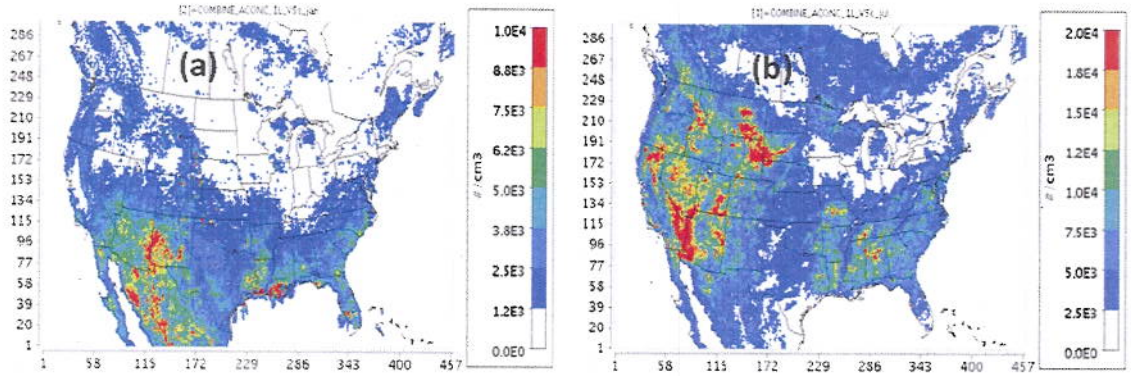

Figure 7: Predicted percentage changes in mean sulfate due to the oxidation of SO_2 by SCI in (a) winter and (b) summer

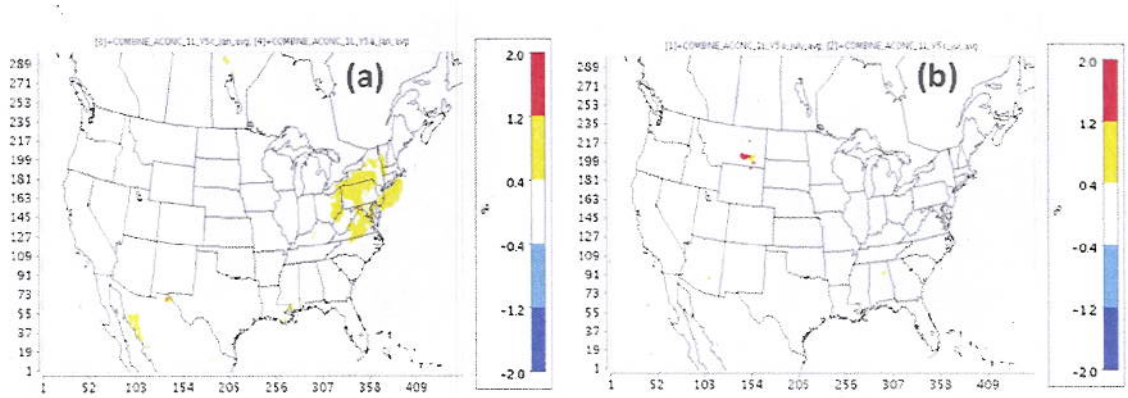

Figure 8: (a) Predicted mean sulfate in summer (10-day average) without the oxidation of SO_2 by SCI (b) changes in mean sulfate due to the oxidation of SO_2 by SCI ($k = 2.4 \times 10^{-15}$ is used for the reaction of SCI and H_2O) (c) changes in mean sulfate due to the oxidation of SO_2 by SCI ($k = 1.0 \times 10^{-16}$ is used for the reaction of SCI and H_2O)

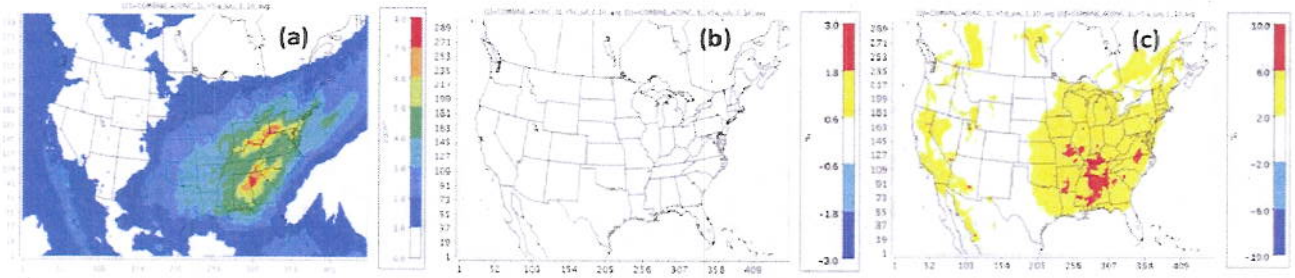

Figure 9: A comparison of predicted NO_2 with and without the aqueous-phase oxidation of S(IV) by NO_2 (higher rate constant) with observed data from the AQS in (a) winter and (b) summer. Model "A" represents predictions without the aqueous-phase oxidation of S(IV) by NO_2, while model "B" represents predictions with the aqueous-phase oxidation of S(IV) by NO_2.

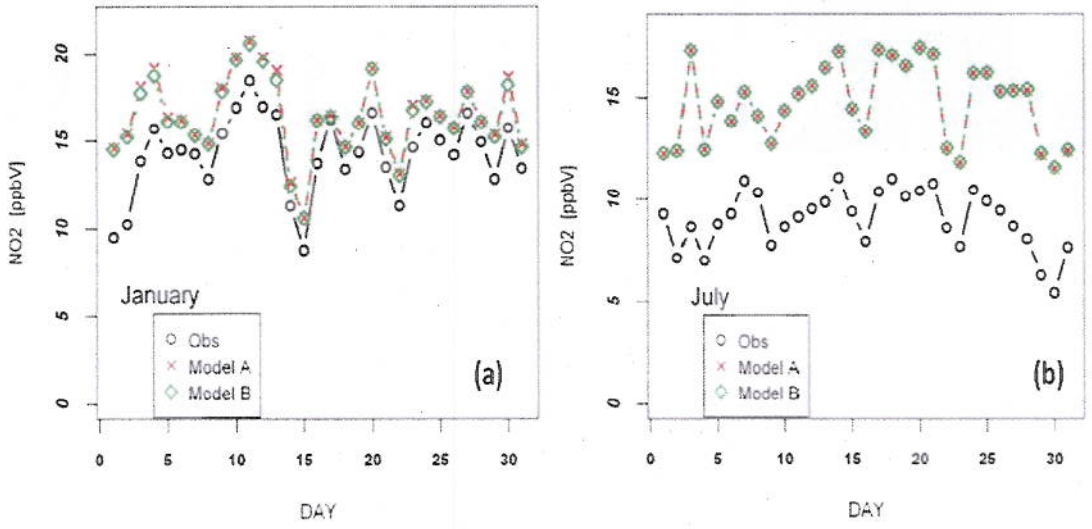

Figure 10: The median and inter-quartile range of observed sulfate from the CASTNet sites, and predicted sulfate with and without the aqueous-phase oxidation of S(IV) by NO_2 (higher rate constant) (a) winter and (b) summer. Model "A" represents predictions without the aqueous-phase oxidation of S(IV) by NO_2, while model "B" represents predictions with the aqueous-phase oxidation of S(IV) by NO_2.

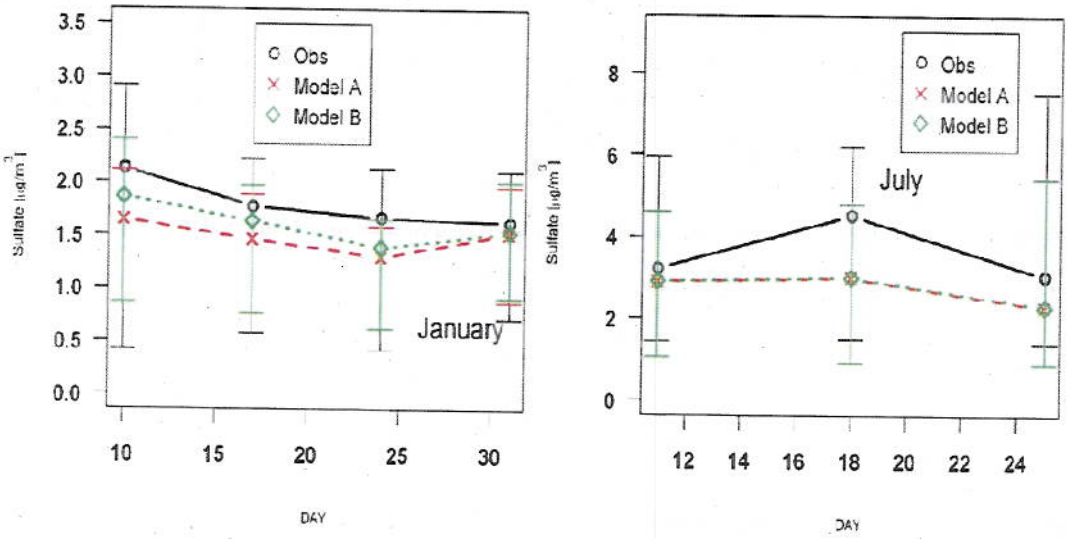

741
742

Table 1: Aqueous-phase sulfur chemistry in CMAQv5.0

Reaction No.	Reaction	Rate constant expression ($M^{-1}s^{-1}$)	Reference
R1	$HSO_3^- + H_2O_2 \rightarrow SO_4^{2-} + H^+$	$k_{R1} = \frac{7.45 \times 10^7 e^{-4990\left(\frac{1}{T} - 0.0\right)}}{1.0 + 13.0\,[H^+]}\,[H^+]$	Jacobson, 1997
R2	$HSO_3^- + MHP \rightarrow SO_4^{2-} + H^+$	$k_{R2} = 1.80 \times 10^7 e^{-4970\left(\frac{1}{T} - 0.0\right)}\,[H^+]$	Jacobson, 1997
R3	$HSO_3^- + PAA \rightarrow SO_4^{2-} + H^+$	$k_{R3} = 700.0 + 8.60 \times 10^7 e^{-4130\left(\frac{1}{T} - 0.0\right)}\,[H^+]$	Jacobson, 1997
R4	$SO_2 + O_3 \rightarrow SO_4^{2-} + 2H^+$	$k_{R4} = 2.40 \times 10^4$	Jacobson, 1997
R5	$HSO_3^- + O_3 \rightarrow SO_4^{2-} + H^+$	$k_{R5} = 8.70 \times 10^6 e^{-5530\left(\frac{1}{T} - 0.0\right)}$	Jacobson, 1997
R6	$SO_3^{2-} + O_3 \rightarrow SO_4^{2-}$	$k_{R6} = 1.50 \times 10^9 e^{-5280\left(\frac{1}{T} - 0.0\right)}$	Jacobson, 1997
R7	$S_{(IV)} + Fe(III)/Mn(II) \rightarrow SO_4^{2-}$	See text	Martin and Goodman, 1991

743
744

Table 2: pH dependent rate constants for the aqueous-phase reaction of S(IV) and NO_2 (Clifton et al., 1988)

pH	Rate constant ($M^{-1}s^{-1}$)
5.3	1.24×10^7
6.7	1.54×10^7
6.8	1.34×10^7
8.7	1.67×10^7
9.3	1.68×10^7
11.8	2.14×10^7
13.0	2.95×10^7

746
747

Table 3: Henry's Law Coefficient (H) of SO_2, H_2O_2, PAA, MHP, O_3, and NO_2 used in CMAQ

Oxidants	Equation for Henry's Law Coefficients	H at 260K ($M\ atm^{-1}$)	H at 270K ($M\ atm^{-1}$)	H at 280K ($M\ atm^{-1}$)	H at 290K ($M\ atm^{-1}$)	H at 300K ($M\ atm^{-1}$)	Reference
H_2O_2	$H = 8.3 \times 10^4 e^{7200\left(\frac{1}{T} - \frac{1}{298}\right)}$	3.1×10^6	1.1×10^6	4.1×10^5	1.6×10^5	7.0×10^4	O'Sullivan et al., 1996
PAA	$H = 8.4 \times 10^2 e^{5300\left(\frac{1}{T} - \frac{1}{298}\right)}$	1.1×10^4	5.3×10^3	2.6×10^3	1.4×10^3	7.5×10^2	O'Sullivan et al., 1996
MHP	$H = 8.1 \times 10^2 e^{5300\left(\frac{1}{T} - \frac{1}{298}\right)}$	4.0×10^3	1.9×10^3	9.5×10^2	5.0×10^2	2.8×10^2	O'Sullivan et al., 1996
NO_2	$H = 1.4 \times 10^{-2} e^{2500\left(\frac{1}{T} - \frac{1}{298}\right)}$	4.1×10^{-2}	2.9×10^{-2}	2.1×10^{-2}	1.5×10^{-2}	1.1×10^{-2}	Chameides, 1984
O_3	$H = 1.14 \times 10^{-2} e^{2300\left(\frac{1}{T} - \frac{1}{298}\right)}$	3.5×10^{-2}	2.5×10^{-2}	1.9×10^{-2}	1.4×10^{-2}	1.1×10^{-2}	Kosak-Channing and Helz, 1983

748
749

750
751

Table 4: Measured SCI yields from alkene-O_3 reactions

Alkene	SCI yield	Reference
Ethene	0.35-0.47	Finlayson-Pitts and Pitts,2000
Propene	0.25-0.44	Finlayson-Pitts and Pitts,2000
t-2-Butene	0.19-0.42	Finlayson-Pitts and Pitts,2000
1-Butene	0.27	Hasson et al., 2001
1-Pentene	0.29	Hasson et al., 2001
1-Octene	0.35	Hasson et al., 2001
Methylene cyclohexane	0.26	Hasson et al., 2001
α–Pinene	0.13	Hatakeyama et al., 1984
β–Pinene	0.25-0.27	Hatakeyama et al., 1984, Hasson et al., 2001
Isoprene	0.26	Hasson et al., 2001

752
753

Table 5: The CB05TU mechanism with the SCI chemistry

Reaction No.	Reaction	Rate constant (cm^3 $molecule^{-1}$ s^{-1})	Note
118	O_3 + OLE = … + 0.319*CRIEGEE	See Yarwood et al. (2005)	OLE represents terminal olefins in CB05TU and has lumping similar to that of OLE1 in SAPRC07. We determined the SCI yield for OLE1 in SAPPRC07 and used it for OLE in CB05TU.
122	O_3 + ETH =… + 0.37*CRIEGEE	See Yarwood et al. (2005)	ETH represents ethene in CB05TU. We used SCI yield for ETHENE in SAPPRC07 and used it for ETH in CB05TU.
126	O_3 + IOLE = … + 0.316*CRIEGEE	See Yarwood et al. (2005)	IOLE represents internal olefins in CB05TU and has lumping similar to that of OLE2 in SAPRC07. We determined SCI yield for OLE2 in SAPPRC07 and used it for IOLE in CB05TU.
143	O_3 + ISOP = … + 0.354*CRIEGEE	See Yarwood et al. (2005)	ISOP represents isoprene in CB05TU. We used the SCI yield for ISOPRENE in SAPPRC07 and used it for ISOP in CB05TU.
146	O_3 + ISPD = … + 0.472*CRIEGEE	See Yarwood et al. (2005)	ISPD represents isoprene reaction product in CB05TU. We used SCI yield for IPRD in SAPPRC07 and used it for ISPD in CB05TU.
151	O_3 + TERP = … + 0.268*CRIEGEE	See Yarwood et al. (2005)	TERP represents monoterpene in CB05TU and has lumping similar to TERP in SAPRC07. We determined SCI yield for TERP in SAPPRC07 and used it for TERP in CB05TU.
173	CRIEGEE + SO_2 = SULF	3.90×10^{-11}	Welz et al., (2012)
174	CRIEGEE + NO_2 = NO_3	7.00×10^{-12}	Welz et al., (2012)
175	CRIEGEE + H_2O =	2.40×10^{-15}	Welz et al., (2012)

754
755

Table 6: Descriptions of the model simulations

Simulation number	Gas-phase chemistry	Aqueous-phase chemistry
1	CB05TU	Five aqueous-phase reactions in CMAQv5.0: Oxidation of S(IV) by H_2O_2, MHP, PAA, O_3, Fe/Mn
2	CB05TU	Six aqueous-phase reactions: reactions in simulation #1 and oxidation of S(IV) by NO_2 with lower k reported by Lee and Schartz (1983)
3	CB05TU	Six aqueous-phase reactions: reactions in simulation #1 and oxidation of S(IV) by NO_2 with higher k reported by Clifton et al. (1988)
4	CB05TU + SCI chemistry	Five aqueous-phase reactions in CMAQv5.0: Oxidation of S(IV) by H_2O_2, MHP, PAA, O_3, Fe/Mn

756
757